

# The Modified Void Nucleation and Growth Model (MNAG) for Damage Evolution in BCC Ta

Jie Chen <sup>1</sup>, Darby J. Luscher <sup>2</sup> and Saryu J. Fensin <sup>1,\*</sup>

<sup>1</sup> Materials Science and Technology Division, Los Alamos National Laboratory, Los Alamos, NM 87545, USA; cjenjie@mail.ustc.edu.cn

<sup>2</sup> The Fluid Dynamics and Solid Mechanics group (T-3), Theoretical Division, Los Alamos National Laboratory, Los Alamos, NM 87545, USA; djl@lanl.gov

\* Correspondence: saryuj@lanl.gov

## Cocks-Ashby Model

Cocks and Ashby derived the following equation for damage evolution assuming the dominant mechanism for void growth to be power-law creep [1,2]:

$$\frac{dD}{dt} = \beta \epsilon_0 \left[ \frac{1}{(1-D)^n} - (1-D) \right] \left( \frac{\sigma_e}{\sigma_0} \right)^n \quad (1)$$

Where D is the damage, namely, void volume fraction,  $\beta$  is a constant ( $\sim 0.6$ ),  $\epsilon_0$  is a parameter that depends exponentially on temperature,  $\sigma_e$  is von Mises equivalent stress,  $\sigma_0$  is a scaling parameter for  $\sigma_e$ , and n is the power-law creep exponent (inverse of strain rate sensitivity). Integration of Eq. 1 yields the following solution:

$$\ln|(1-D)^{n+1} - 1| - \ln|(1-D_0)^{n+1} - 1| = (n+1)\epsilon_0\beta t \quad (2)$$

Based on Eq. (2), assuming initial damage  $D_0 = 2 \times 10^{-5}$  (same as the initial damage in MD), for different choices of power-law creep exponent n, along with the other parameters, the resulting damage evolution is plotted in Fig. S1 as compared to MD results for single-crystal Ta along [001] orientation. Cocks-Ashby model predicts a gradual increase in damage accumulation until D reaches  $\sim 0.1$ , and then rises exponentially and instantly [3]. This is rather different from the trend calculated by MD simulations that show a steady increase in the void volume fraction following an initial exponential growth.

**Citation:** Chen, J.; Luscher, D.; Fensin, S. A Modified Void Nucleation and Growth Model (MNAG) for Damage Evolution in BCC Ta. *Appl. Sci.* **2021**, *11*, 3378. <https://doi.org/10.3390/app11083378>

Academic editor: Alberto Campagnolo

Received: 18 February 2021

Accepted: 4 April 2021

Published: 9 April 2021

**Publisher's Note:** MDPI stays neutral with regard to jurisdictional claims in published maps and institutional affiliations.



**Copyright:** © 2021 by the authors. Submitted for possible open access publication under the terms and conditions of the Creative Commons Attribution (CC BY) license (<http://creativecommons.org/licenses/by/4.0/>).

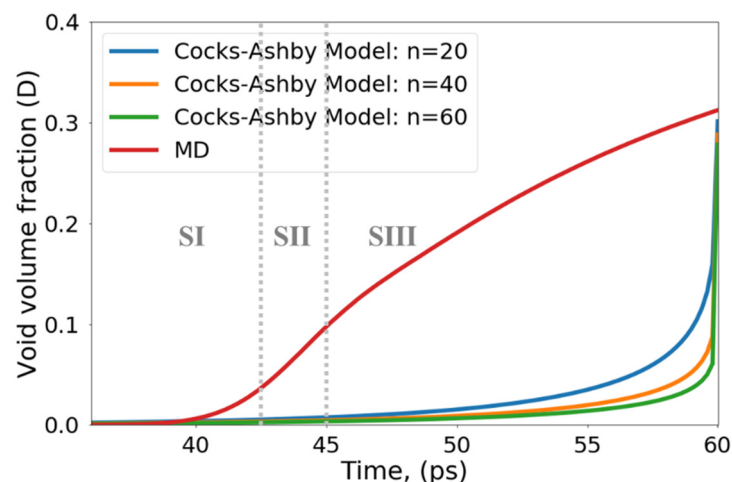


**Figure S1.** Damage (void volume fraction) evolution based on Cocks-Ashby model with different choices of n, as compared to MD results for [001] single-crystal Ta. For the sake of comparison with MD, the starting time is set at 36 ps for both model. This is also void nucleation time in MD.

### Meyer-JMAK Treatment

Meyers et al. proposed a void growth kinetics based on Curran-Seaman-Shockey (CSS) theory [4,5] and Johnson-Mehl-Avrami-Kolmogorov (JMAK) equations [3,6-10], referred to as Meyer-JMAK treatment here. For intergranular void nucleation and growth, they derived the following equation for damage evolution, assuming exponential dependence of void nucleation rate on tensile stress and exponential increase of void growth rate with time:

$$D = 1 - \exp \left[ -\frac{4}{3} \pi \dot{N}_o e^{\frac{\sigma - \sigma_{n0}}{\sigma_c}} k^3 \phi(t) \right] \quad (3)$$

And

$$k = \frac{\sigma - \sigma_{g0}}{4\eta} \quad (4)$$

$$\phi(t) = \frac{1}{3k} \left[ \frac{2}{9k^3} + e^{3kt} \left( t^3 - \frac{t^2}{k} + \frac{2t}{3k^2} - \frac{2}{9k^3} \right) \right] \quad (5)$$

where  $\sigma$  is the tensile stress,  $\sigma_{n0}$  is the void nucleation threshold,  $\sigma_{g0}$  is the void growth threshold,  $\dot{N}_o$  is base void nucleation rate,  $\eta$  is material viscosity, and  $\sigma_c$  is a parameter that dictates the exponential dependence of void nucleation rate upon stress. With the choice of the following parameters:  $\sigma = 10$  GPa,  $\sigma_{n0} = 8$  GPa,  $\sigma_c = 0.2$  GPa,  $\sigma_{g0} = 5$  GPa, and by varying base void nucleation rate  $\dot{N}_o$ , the damage evolution as plotted in Fig. S2 suggests an ever-increasing void growth rate as  $k$  needs always to be positive, and Eq. (4) only yields meaningful results under such condition. As such, the Meyer-JMAK treatment can describe void nucleation and growth quite well, for example, the predicted evolution matches well with that of MD at  $\dot{N}_o = 7 \times 10^{-7} \text{ m}^{-3} \text{ s}^{-1}$  till  $\sim 45$  ps, after which coalescence becomes significant and results in disparity with MD results. Such behavior is similar to the original NAG model, as they both are based on Curran-Seaman-Shockey (CSS) theory. Different choices of the other parameters do not alter the shape of the curve in Fig. S2.

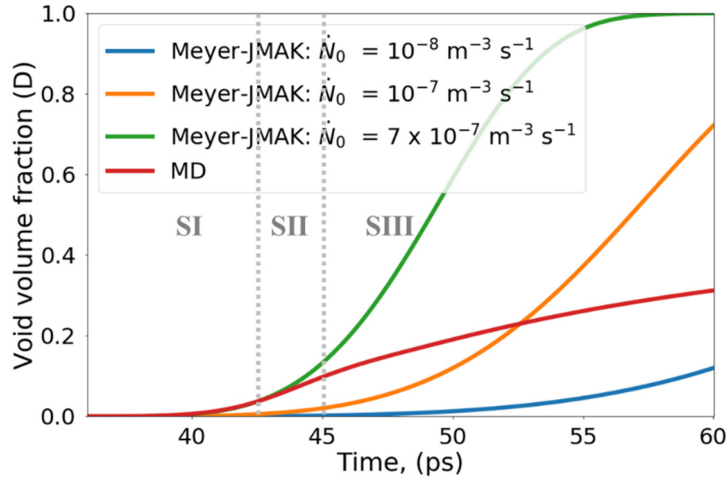


**Figure S2.** Damage (void volume fraction) evolution based on Meyer-JMAK treatment, with different choices of  $\dot{N}_o$ , as compared to MD results for [001] single-crystal Ta.

### Critical void volume fraction prior to coalescence

First, using a simple analysis, we show that void coalescence inevitably takes place when void volume fraction reaches  $\sim 0.15$ , assuming a homogenous distribution of voids. Assume  $N$  spherical voids of a radius  $R$  distributed homogeneously in the system with a volume of  $V$ , the total volume of voids is then:

$$V_v = N * \frac{4}{3} \pi R^3 \quad (6)$$

Previously, Seppala et al. have observed that if one assumes void coalescence is initiated through the interaction of the plastic field of neighboring voids (which holds for Ta), then this interaction would cause the voids to grow in an anisotropic manner prior to final coalescence. By studying the growth of a two-void system in Cu (with the same radius  $R$ ), they found that regardless of strain rate, when the separation between the void surfaces  $R_L$  reaches  $R$ , the voids start growing in an anisotropic manner, which then leads to void coalescence in one orientation [11]. Assuming that this criterion holds for Ta as well, in the extreme case of full occupation of voids, with a void surface separation of  $R_L$ , in the entire system, the total volume occupied by the voids  $V_V^{Full}$  is then:

$$V_V^{Full} = N * \left[ 2 * \left( R + \frac{R_L}{2} \right) \right]^3 \quad (7)$$

Void coalescence is dominant when  $V_V^{Full} = V$ . Combining the above two equations, then the critical void volume fraction  $D_{crit}$  is:

$$D_{crit} = \frac{V_V}{V_V^{Full}} = \frac{N * \frac{4}{3} \pi R^3}{N * \left[ 2 * \left( R + \frac{R_L}{2} \right) \right]^3} \quad (8)$$

Assuming  $R_L = R$ , and substituting it into the above equation, one obtains  $D_{crit} = \frac{4\pi}{81} = 0.155$ . This critical volume fraction is very close to the value (0.15) [12].

In the case of [001] single-crystal Ta, such a critical void volume fraction is reached at a time of ~48 ps. However, due to the inhomogeneous nature of void nucleation in Ta (due to extensive dislocation slip and twinning activity), void coalescence is expected to set in and contribute before the critical void volume fraction is reached. Thus, it is necessary to incorporate void coalescence explicitly in the damage model to not only represent the MD data but also to capture the three stages of damage: nucleation, growth and coalescence.

### Microstructure Evolution

The snapshots of the [001] single-crystal Ta during SI, SII and SIII are shown in Fig. S3. The number density of voids peak at 42.6 ps (end of SI) is shown in Fig. S3a. At this stage, despite a high number density of voids, most of the voids are isolated and remain small in size. The nucleated voids grow significantly under the high tensile stress in the system, as shown in in Fig. S3b at 45 ps (SII). The continual growth of existing voids as shown in Fig. S3c at 48 ps (end of SII) results in voids coming into contact with each other and eventually coalesce. Such coalescence results in the final spall plane as shown in Fig. S3d at 60 ps (SIII), where most of the voids in the spall region coalesce into one, resulting in the fracture of the system.

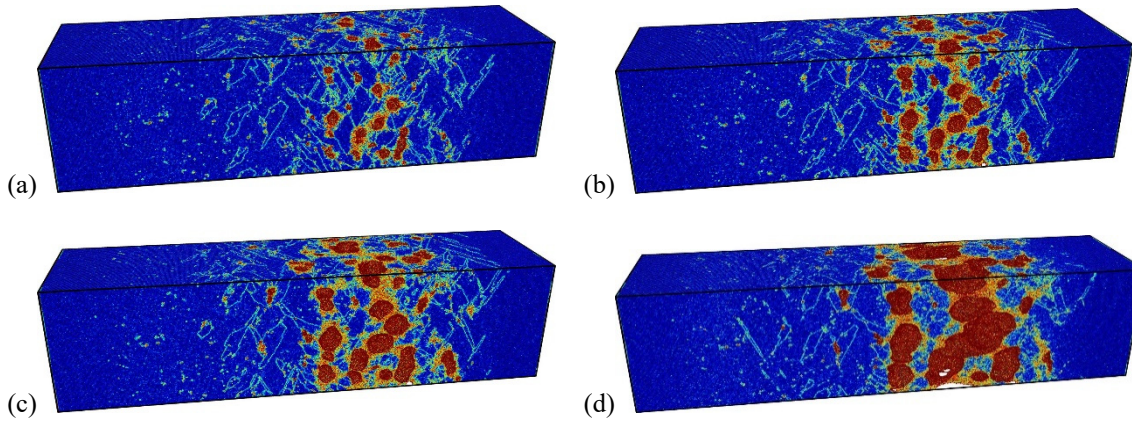


**Figure S3.** Snapshots of [001] single-crystal Ta at different times: (a) 42.6 ps, (b) 45 ps, (c) 48 ps, (d) 60 ps. The atoms are colored based on centrosymmetry parameters.

### Effects of time step $\Delta t$

To investigate the effect of time step  $\Delta t$  during MD simulations on the above results, the MNAG model is integrated at a time step of 0.002 ps, 0.02 ps, 0.2 ps and 2 ps for a time period of 1000 ps for [001] single-crystal Ta. The resulting evolution of number density and volume fraction of voids are plotted in Fig. S4. The overall void evolution is very similar for a time step of 0.002 ps, 0.02 ps and 0.2 ps. However, a slight deviation is observed when the time step is increased to 2 ps. As a result, a choice of 0.2 ps for the time step in this work is small enough to achieve convergence.

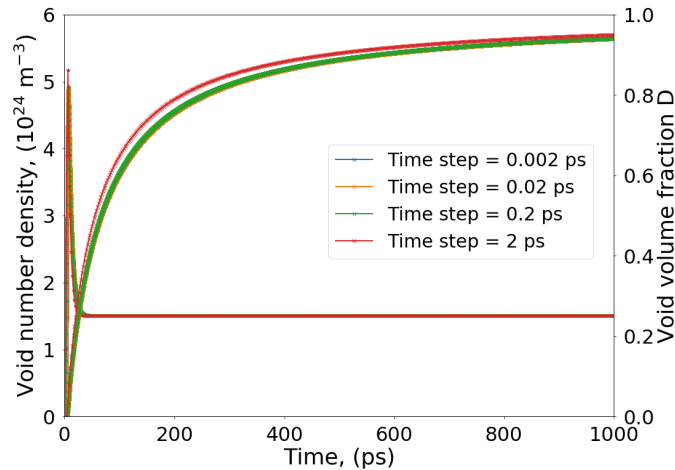


**Figure S4.** Evolution of number density and volume fraction of voids for [001] single-crystal Ta based on MNAG model over a period of 1000 ps for time steps varying from 0.002 ps to 2 ps.

### Reference

1. Cocks, A.C.F.; Ashby, M.F. Intergranular Fracture during Power-law Creep under Multiaxial Stresses. *Met. Sci.* **1980**, *14*, 395–402, doi:10.1179/030634580790441187.
2. Cocks, A.; Ashby, M. On Creep Fracture by Void Growth. *Prog. Mater. Sci.* **1982**, *27*, 189–244, doi:10.1016/0079-6425(82)90001-9.
3. Remington, T.; Hahn, E.; Zhao, S.; Flanagan, R.; Mertens, J.; Sabbaghianrad, S.; Langdon, T.; Wehrenberg, C.; Maddox, B.; Swift, D.; et al. Spall Strength Dependence on Grain Size and Strain Rate in Tantalum. *Acta Mater.* **2018**, *158*, 313–329, doi:10.1016/j.actamat.2018.07.048.
4. Curran, D.R.; Seaman, L.; Shockey, D.A. Dynamic Failure in Solids. *Phys. Today* **1977**, *30*, 46, doi:10.1063/1.3037367.
5. Seaman, L.; Curran, D.R.; Shockey, D.A. Computational Models for Ductile and Brittle Fracture. *J. Appl. Phys.* **1976**, *47*, 4814–4826, doi:10.1063/1.322523.
6. Avrami, M. Kinetics of Phase Change. I General Theory. *J. Chem. Phys.* **1939**, *7*, 1103–1112, doi:10.1063/1.1750380.
7. Avrami, M. Kinetics of Phase Change. II Transformation-Time Relations for Random Distribution of Nuclei. *J. Chem. Phys.* **1940**, *8*, 212–224, doi:10.1063/1.1750631.
8. Avrami, M. Granulation, Phase Change, and Microstructure Kinetics of Phase Change. III. *J. Chem. Phys.* **1941**, *9*, 177–184, doi:10.1063/1.1750872.
9. Johnson, W.A.; Mehl, R.F. Reaction Kinetics in Processes of Nucleation and Growth. *Trans. Metall. Soc. AIME* **1939**, *135*, 416–442.
10. Kolmogorov, A.N. On the Statistical Theory of the Crystallization of Metals. *Bull. Acad. Sci. USSR Math. Ser* **1937**, *1*, 355–359.
11. Seppälä, E.T., Belak, J., Rudd, R.E., 2004. Onset of Void Coalescence during Dynamic Fracture of Ductile Metals. *Phys. Rev. Lett.* **93**, 245503.
12. Tvergaard, V., Needleman, A., 1984. Analysis of the cup-cone fracture in a round tensile bar. *Acta Metallurgica* **32**, 157–169.